

Trajectory Representation Learning on Road Networks and Grids with Spatio-Temporal Dynamics

Stefan Schestakov

L3S Research Center, Leibniz University Hannover
Hannover, Germany
schestakov@L3S.de

Simon Gottschalk

L3S Research Center, Leibniz University Hannover
Hannover, Germany
gottschalk@L3S.de

ABSTRACT

Trajectory representation learning is a fundamental task for applications in fields including smart city, and urban planning, as it facilitates the utilization of trajectory data (e.g., vehicle movements) for various downstream applications, such as trajectory similarity computation or travel time estimation. This is achieved by learning low-dimensional representations from high-dimensional and raw trajectory data. However, existing methods for trajectory representation learning either rely on grid-based or road-based representations, which are inherently different and thus, could lose information contained in the other modality. Moreover, these methods overlook the dynamic nature of urban traffic, relying on static road network features rather than time-varying traffic patterns. In this paper, we propose TIGR, a novel model designed to integrate grid and road network modalities while incorporating spatio-temporal dynamics to learn rich, general-purpose representations of trajectories. We evaluate TIGR on two real-world datasets and demonstrate the effectiveness of combining both modalities by substantially outperforming state-of-the-art methods, i.e., up to 43.22% for trajectory similarity, up to 16.65% for travel time estimation, and up to 10.16% for destination prediction.

1 INTRODUCTION

Trajectories, i.e., sequences of locations representing agent movements over time, are increasingly prevalent due to widespread location-aware devices. This abundance of trajectory data has surged research in trajectory data analysis, including trajectory similarity computation [6], destination prediction [18], and travel time estimation [14, 40].

A fundamental task of trajectory analysis is *Trajectory Representation Learning (TRL)*, which aims to learn low-dimensional and meaningful representations of trajectories from high-dimensional and raw trajectory data. TRL facilitates the utilization of trajectory data for various downstream applications without the need for manual feature engineering and unique models for specific tasks.

Raw trajectory data often suffers from noise, sparsity, and spatio-temporal irregularities. TRL methods address these issues using either grid or road network discretization, representing trajectories

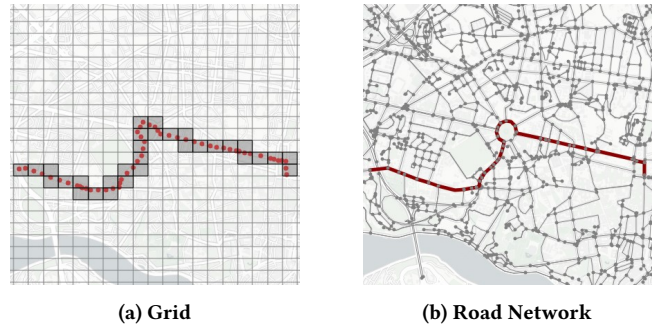


Figure 1: Trajectory represented by grid cells (a) and by road segments on a road network (b). © OpenStreetMap, © Carto.

as sequences of grid cells (Figure 1a) or road segments (Figure 1b). Existing TRL methods fall into one of these categories:

- **Grid-based methods** [2, 17] divide the spatial domain into a regular grid of equal-sized cells, and encode a trajectory as a sequence of these cells. This symmetric, uniform structure is well suited to preserve spatial and structural properties, including shape, distance, and direction.
- **Road-based methods** [13, 36] represent a trajectory by mapping its locations onto a road network and obtaining a sequence of road segments. Road-based methods inherently model motion restrictions and can exploit knowledge contained in road networks, such as traffic, road features, and topology.

Both modalities are inherently different, thus, capturing different trajectory characteristics and possessing unique advantages. However, current TRL methods rely solely on one of both modalities and under this restriction could fail to capture vital information on trajectories and lead to inferior representations. Moreover, there is a lack of comparative studies between both modalities. So far, TRL methods have merely adapted methods of the other modality to their modality, by using road-sequences instead of grid-sequences as input and vice versa [13, 17]. Thus, there is an insufficient understanding of each modality’s respective advantages.

Further, we observe that current TRL methods largely neglect spatio-temporal dynamics. Although recent approaches incorporate temporal data, they still treat the road network as static [13, 36]. This limitation prevents the extraction of crucial spatio-temporal patterns, such as drastically changing traffic conditions during peak hours. These dynamics greatly influence downstream applications such as travel time estimation, highlighting the need to incorporate spatio-temporal dynamics in TRL approaches.

Permission to make digital or hard copies of all or part of this work for personal or classroom use is granted without fee provided that copies are not made or distributed for profit or commercial advantage and that copies bear this notice and the full citation on the first page. Copyrights for components of this work owned by others than ACM must be honored. Abstracting with credit is permitted. To copy otherwise, or republish, to post on servers or to redistribute to lists, requires prior specific permission and/or a fee. Request permissions from permissions@acm.org.

Conference’17, July 2017, Washington, DC, USA

© 2024 Association for Computing Machinery.

ACM ISBN 978-x-xxxx-xxxx-x/YY/MM... \$15.00

<https://doi.org/10.1145/nnnnnnn.nnnnnnn>

In this paper, we propose TIGR — a framework for **TRL** Integrating **Grid** and **Road** network modalities with spatio-temporal dynamics. Based on our previous observations, we identify two main challenges: (1) *Heterogeneity between grid and road modality*. Both modalities use fundamentally different spatial discretization, making it challenging to directly combine or fuse both types of information. (2) *Spatio-temporal dynamics*. Urban traffic is highly dynamic and varies significantly across time and space. Modeling those dynamics effectively is highly challenging.

To address these challenges, TIGR employs a three-branch architecture that processes grid data, road network data, and spatio-temporal dynamics in parallel. The grid and road branches represent our two primary modalities, while the spatio-temporal branch extracts dynamic traffic patterns derived from the road modality. We embed each branch into latent trajectory representations and align representations within (intra-modal) and across (inter-modal) the distinct branches. By combining these three components, TIGR facilitates a more sophisticated extraction of diverse trajectory characteristics. This integrated approach allows our model to leverage the strengths of both grid-based and road-based methods while also accounting for the dynamic nature of urban traffic.

We validate the effectiveness of TIGR on two real-world datasets and three downstream tasks. Our approach outperforms state-of-the-art TRL methods across all settings, demonstrating the effectiveness of combining road and grid modalities for trajectory embeddings. In summary, the main contributions of this paper are:

- We propose TIGR¹, a novel TRL model designed to integrate grid and road network modalities, outperforming TRL methods across multiple downstream tasks.
- We develop a novel Spatio-Temporal Extraction method, enabling TIGR to extract traffic patterns and temporal dynamics.
- We leverage a three-branch architecture to process grid data, road network data, and spatio-temporal dynamics in parallel and align all three branches through an inter- and intra-modal contrastive loss.
- To the best of our knowledge, we conduct the first study to compare road-based and grid-based TRL methods across various downstream tasks, revealing that each modality exhibits distinct strengths in different applications.

2 RELATED WORK

Trajectory Representation Learning (TRL) encodes raw spatio-temporal data into a compact feature vector, capturing essential trajectory characteristics. TRL methods can be categorized into *grid-based* and *road-based* methods.

Grid-based TRL A grid divides the spatial domain into a regular grid, which preserves structural and spatial concepts and thus is used in many spatio-temporal tasks, such as traffic prediction [25], spatial representation learning [20] and remote sensing [12, 31]. Grid-based TRL methods augment trajectories, e.g., by downsampling or distortion, and reconstruct the original trajectory (t2vec [15]) or contrast augmented views with contrastive learning

(CLT-Sim [7]). Recent methods further leverage Transformer networks and add auxiliary information, such as temporal regularities (CSTTE [17]) or extracted location features (TrajCL [2]).

Road-based TRL Map matching algorithms allow trajectories to be represented as sequences of road segments in a road network [3]. Additionally, road network representation learning [29, 30] facilitates leveraging the road network topology and semantics to learn more meaningful trajectory representations. Road-based TRL methods utilize different training paradigms: Trembr [8] utilizes an RNN-based encoder-decoder model and reconstructs the input trajectory. PIM [34] captures local and global information leveraging curriculum learning. Toast [5] predicts previously masked tokens. MMTEC [16] and JGRM [19] leverage GPS points to extract more detailed trajectory characteristics. START [13] combines masked token prediction with contrastive learning. LightPath [36] utilizes sparse paths to reduce model complexity.

In contrast to these related works, TIGR combines both modalities to facilitate a more intricate extraction of various trajectory characteristics and incorporates the modeling of spatio-temporal dynamics, which has largely been neglected.

3 PROBLEM DEFINITION

Definition 3.1. (Trajectory) A trajectory represents the movement of an agent recorded by a GPS-enabled device. Formally, a trajectory can be denoted as $\mathcal{T} = [(x_i, y_i, t_i)]_{i=1}^{|\mathcal{T}|}$, where (x_i, y_i) is the location represented as a spatial coordinates pair and t_i is the timestamp of the location at time step i . $|\mathcal{T}|$ is the length of the trajectory, and varies for different trajectories.

Grid-based methods model trajectories by first defining a grid over the spatial domain (e.g., representing a city) and then mapping each point onto its corresponding grid cell.

Definition 3.2. (Grid) A grid is a regular partition of the spatial domain into $M \times N$ cells. Each cell has a unique pair of indices (m, n) , where $m \in \{1, \dots, M\}$ and $n \in \{1, \dots, N\}$. The set of all grid cells is denoted by \mathcal{C} , where $\mathcal{C} = \{c_1, c_2, \dots, c_{|\mathcal{C}|}\}$ and each c_i is associated with a unique pair of indices (m, n) .

Definition 3.3. (Grid-based Trajectory) A grid-based trajectory $\mathcal{T}^g = [(c_i, t_i)]_{i=1}^{|\mathcal{T}^g|}$ represents a trajectory as a sequence of grid cells, where each c_i denotes a grid cell in the grid \mathcal{C} .

Road-based methods model trajectories based on a road network by mapping each point onto the road network using a map matching algorithm [32].

Definition 3.4. (Road Network) We define a road network as a directed graph $G = (\mathcal{V}, \mathcal{A}, \mathcal{F})$. \mathcal{V} is a set of nodes, where each node $v_i \in \mathcal{V}$ represents a road segment. \mathcal{A} is the adjacency matrix, where $\mathcal{A}_{ij} = 1$ implies that a road segment v_j is directly accessible from road segment v_i , and $\mathcal{A}_{ij} = 0$ otherwise. A road network has a feature set $\mathcal{F} \in \mathbb{R}^{|\mathcal{V}| \times f}$ representing road segment features with dimension f .

Definition 3.5. (Road-based Trajectory) A road-based trajectory $\mathcal{T}^r = [(v_i, t_i)]_{i=1}^{|\mathcal{T}^r|}$ represents a trajectory constrained by a road network G , where each $v_i \in \mathcal{V}$ denotes a road segment in the road network $G = (\mathcal{V}, \mathcal{A}, \mathcal{F})$.

¹The code will be published upon acceptance

Problem Statement. Given a set of trajectories $\mathcal{D} = \{\mathcal{T}_i\}_{i=1}^{|\mathcal{D}|}$, the task of trajectory representation learning is to learn a trajectory encoder $F : \mathcal{T} \mapsto \mathbf{z}$ that embeds a trajectory \mathcal{T} into a general-purpose representation $\mathbf{z} \in \mathbb{R}^d$ with dimension d . The representation \mathbf{z} should accurately represent \mathcal{T} suitable for various downstream applications, such as trajectory similarity computation, travel time estimation and destination prediction. To this end, the trajectory encoder is trained in an unsupervised fashion.

4 TIGR APPROACH

In this section, we present TIGR’s training procedure, which aims to produce similar representations between two masked views of the same data instance and between the same data instances across different modalities.

As depicted in Figure 2, TIGR integrates two primary modalities, grid and road, along with a dedicated spatio-temporal component derived from the road modality. Thus, our architecture consists of three parallel branches processing grid, road network, and spatio-temporal dynamics respectively. Each branch embeds a trajectory \mathcal{T} into a sequence of token embeddings, thus obtaining \mathbf{T}^g , \mathbf{T}^r and \mathbf{T}^{st} . We leverage distinct embedding layers for \mathbf{T}^g and \mathbf{T}^r to capture the structural properties of both modalities. The spatio-temporal component, on the other hand, aims to extract traffic patterns and temporal dynamics and is detailed in the next section. Subsequently, we apply masking to each branch to obtain distinct views and embed each view of each branch using a modality-agnostic encoder. The objective is then to align the representations within each branch (intra-modal loss) and across branches (inter-modal loss).

4.1 Spatio-Temporal Extraction

Modeling spatio-temporal dynamics is crucial for effective TRL. However, current methods neglect temporal information completely [7, 36], or include temporal information, but solely model static road features [13, 16]. Thus, these approaches fail to capture the dynamic nature of traffic patterns changing over time. To address this limitation, we propose a novel spatio-temporal extraction method that effectively models both — dynamic traffic patterns and temporal regularities.

Our approach consists of three main components: dynamic traffic embedding, temporal embedding, and fusion via local multi-head attention. First, we develop a dynamic traffic embedding that captures changing traffic conditions across different times of day and days of the week, using graph convolutions over transition probabilities to model traffic flow patterns. Second, we introduce a temporal embedding that allows our model to capture recurring temporal patterns (e.g., daily rush hours, weekly trends) and temporal dependencies. Finally, we fuse those embeddings by proposing the local multi-head attention (LMA), based on the observation that traffic within a small spatial and temporal window tends to be very similar, while traffic on distant roads or at different times can differ significantly. Our idea is to leverage the multiple heads used in multi-head attention to perform local attention over short sequences. This approach of spatio-temporal extraction enables TIGR to learn rich representations that account for the complex, time-varying nature of urban traffic.

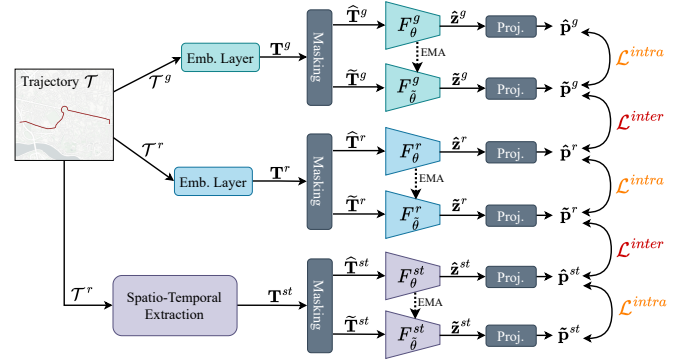


Figure 2: Framework of TIGR’s training procedure.

4.1.1 Dynamic Traffic Embedding. To capture dynamic traffic behavior and traffic flow, we leverage graph convolutions over transition probabilities. Let $X \in \mathcal{R}^{|\mathcal{V}| \times |\mathcal{V}|}$ be the aggregated traffic matrix, containing mean traffic speeds for each weekday t_d and each hour t_h . Further, $P \in \mathcal{R}^{|\mathcal{V}| \times |\mathcal{V}|}$ is the transition probability matrix between connected road segments based on the frequency of trajectories passing through them. For two connected road segments v_i and v_j , the transition probability is given by $P_{[i,j]}$ and is calculated from historical trajectories,

$$P_{[i,j]} = \frac{\#transitions(v_i \rightarrow v_j) + 1}{\#total_visits(v_i) + |\mathcal{N}(v_i)|}, \quad (1)$$

where $|\mathcal{N}(v_i)|$ is the number of v_i ’s neighbors. To leverage P for graph convolutions, we further add self-loops and normalize, i.e., $P' = D^{-1}(P + I)$, where D is the degree matrix and I the identity matrix. Formally, the transition probability weighted graph convolution is then defined by:

$$\mathbf{h}_i = P'_{[i,i]} w_i \mathbf{x}_i^{(t_d, t_h)} + \sum_{v_j \in \mathcal{N}(v_i)} P'_{[i,j]} w_j \mathbf{x}_j^{(t_d, t_h)}, \quad (2)$$

where \mathcal{N} is the neighbor function returning all neighbors of a road, w ’s are learnable parameters, $\mathbf{x}^{(t_d, t_h)} \in X$ is the traffic state at weekday t_d and hour t_h , and \mathbf{h}_i is the dynamic traffic embedding of road segment v_i . Given the sequence of roads in \mathcal{T}^r , we obtain the sequence of dynamic traffic embeddings $\mathbf{T}^s = (\mathbf{h}_1, \mathbf{h}_2, \mathbf{h}_3, \dots, \mathbf{h}_{|\mathcal{T}^r|})$.

4.1.2 Temporal Embedding. Inspired by the sinusoidal Positional Embeddings [27], we learn time embeddings by utilizing the cosine function to capture periodic behavior. Let t_i be the i -th time point in a trajectory, then we obtain its time embedding \mathbf{t}_i :

$$\mathbf{t}_i[k] = \begin{cases} w_k t_i + \phi_k & \text{if } k = 0, \\ \cos(w_k t_i + \phi_k) & \text{else,} \end{cases} \quad (3)$$

where $\mathbf{t}_i[k]$ is the k -th element of the embedding vector $\mathbf{t}_i \in \mathbb{R}^q$ with dimension q , and w_k and ϕ_k are learnable parameters. This representation of time allows periodic behaviors to be captured through the cosine activation function and non-periodic patterns through the linear term. Then, we define the sequence of temporal embeddings of a trajectory \mathcal{T}^r as $\mathbf{T}^t = (\mathbf{t}_1, \mathbf{t}_2, \mathbf{t}_3, \dots, \mathbf{t}_{|\mathcal{T}^r|})$.

4.1.3 Fusion via Local Multi-Head Attention. First, we propose the local multi-head attention, which aims to leverage each individual head to perform a local attention over a specific subsequence. Let $\mathbf{T} \in \mathbb{R}^{|\mathbf{T}| \times d}$ be the input with sequence length $|\mathbf{T}|$ and dimension d . For each head $h \in 1, \dots, H$, we split \mathbf{T} into H subsequences along the sequence dimension, i.e., $\mathbf{T}_h \in \mathbb{R}^{|\mathbf{T}|/H \times d}$, and project each \mathbf{T}_h into query, key and value matrices:

$$Q_h = \mathbf{T}_h W_h^Q, K_h = \mathbf{T}_h W_h^K, V_h = \mathbf{T}_h W_h^V, \quad (4)$$

where $W_h^Q, W_h^K, W_h^V \in \mathbb{R}^{d \times d}$ are the weight matrices. Next, we apply the standard attention mechanism for each head:

$$Att_h(Q_h, K_h, V_h) = \text{softmax}\left(\frac{Q_h K_h^T}{\sqrt{d}}\right) V_h. \quad (5)$$

Finally, we define the local multi-head attention (LMA) as the concatenation of each attention head along the sequence dimension and a projection with the weight matrix W^O :

$$LMA(Q, K, V) = [Att_1 || Att_2 || \dots || Att_{|H|}] W^O. \quad (6)$$

To fuse the dynamic traffic and temporal embeddings, we leverage cross-attention utilizing the previously proposed LMA and a concatenation operation:

$$\mathbf{T}^{st} = LMA(\mathbf{T}^s, \mathbf{T}^t, \mathbf{T}^t) || LMA(\mathbf{T}^t, \mathbf{T}^s, \mathbf{T}^s). \quad (7)$$

This allows both embeddings to attend to the other and to learn more intricate correlations between dynamic traffic and time periodicity through local attention.

4.2 Masking

After embedding each branch, we obtain a sequence of token embeddings \mathbf{T}^b for each of the branches $b \in \{g, r, st\}$. Next, we apply masking by randomly dropping some of the tokens and obtain two distinct views for each branch: $\tilde{\mathbf{T}}^b$ (View 1) and $\bar{\mathbf{T}}^b$ (View 2). The role of masking is twofold. First, we obtain two different views of the same data instance to guide the contrastive learning within each branch. Second, similar to how masked autoencoders (MAE) [11] learn representations, the encoder has to develop an understanding of spatial relationships and learn intrinsic information about the trajectory, i.e., the underlying route. We investigate three masking strategies:

- **Random masking (RM):** We randomly select a subset of tokens in a trajectory \mathbf{T}^b , based on the share $p_{RM} \in (0, 1)$, and mask (i.e., drop) them.
- **Consecutive masking (CM):** We mask a consecutive amount of points within the trajectory, where the amount of points is defined by the share $p_{CM} \in (0, 1)$.
- **Truncation (TC):** Similarly, we mask consecutive points from the origin or destination of a trajectory \mathbf{T}^b , leading to a truncation of the trajectory. We apply $p_{TC} \in (0, 1)$ to define the share.

4.3 Encoder

The encoder transforms each masked trajectory into a low-dimensional embedding. Our approach employs two types of encoders: a target encoder $F_\theta^b(\cdot)$ that encodes $\tilde{\mathbf{T}}^b$ into $\hat{\mathbf{z}}^b \in \mathbb{R}^d$, and an anchor

encoder $F_{\tilde{\theta}}^b(\cdot)$ that encodes $\bar{\mathbf{T}}^b$ into $\tilde{\mathbf{z}}^b \in \mathbb{R}^d$. Both encoders have different parameters, where the target encoder's parameters $\tilde{\theta}$ are updated using an exponential moving average (EMA) of the anchor encoder's parameters θ : $\tilde{\theta} \leftarrow \mu \tilde{\theta} + (1 - \mu)\theta$, where $\mu \in [0, 1]$ is a target decay rate. This EMA update ensures a more stable learning target and prevents representation collapse [1].

For the encoder architecture, we base our design on the Transformer [27] with specific enhancements. We incorporate Rotary Positional Embeddings (RoPE) [26], which capture relative positional information during the attention process, improving upon standard positional embeddings that only represent absolute positions. Additionally, we utilize Root Mean Square Layer Normalization (RMSNorm) [38] and apply it before the multi-head attention and feed-forward layers, rather than after. This modification further stabilizes the training process. These architectural choices enable our encoders to effectively capture the complex spatial and temporal relationships within trajectory data.

4.4 Inter- and Intra-Modal Losses

Next, we project each representation through a *projection head*, modeled as an MLP. After projection of $\hat{\mathbf{z}}^b$ and $\tilde{\mathbf{z}}^b$, we obtain $\tilde{\mathbf{p}}^b$ and $\hat{\mathbf{p}}^b$. We propose to employ the contrastive objective within each branch (intra-modal) and across branches (inter-modal) to learn rich and diverse representations that capture complementary information from both modalities and the spatio-temporal component. For the contrastive objective, we leverage the InfoNCE loss [23]:

$$\mathcal{L}(x, y) = -\log \frac{\exp(x \cdot y / \tau)}{\sum_{j=0}^{|\mathcal{Q}_{neg}|} \exp(x \cdot y_j / \tau) + \exp(x \cdot y / \tau)}, \quad (8)$$

where τ is the temperature parameter, and \mathcal{Q}_{neg} is the negative sample queue, updated at each iteration to maintain a large set of negative samples. Then we align views within each branch (intra-modal) and across distinct branches (inter-modal):

Intra-modal contrastive learning enables alignment *within* each branch. We contrast the projected embeddings within each branch leveraging the contrastive loss from Eq. 8:

$$\mathcal{L}^{intra} = 1/3 \sum_{m \in \{g, r, st\}} \mathcal{L}(\tilde{\mathbf{p}}^m, \hat{\mathbf{p}}^m). \quad (9)$$

Inter-modal contrastive learning facilitates alignment *across* each branch. We contrast the projections of both structural branches, i.e., $\tilde{\mathbf{p}}^g$ and $\hat{\mathbf{p}}^r$, as well as both road network-modality based branches², i.e., $\tilde{\mathbf{p}}^r$ and $\hat{\mathbf{p}}^{st}$. We define the inter-modal loss as:

$$\mathcal{L}^{inter} = 1/2 [\mathcal{L}(\tilde{\mathbf{p}}^g, \hat{\mathbf{p}}^r) + \mathcal{L}(\tilde{\mathbf{p}}^r, \hat{\mathbf{p}}^{st})]. \quad (10)$$

These contrastive losses promote the alignment within and across branches. The overall loss function of TIGR is the weighted sum of the inter and intra loss, with λ being a weighting coefficient:

$$\mathcal{L}_{TIGR} = \lambda \mathcal{L}^{intra} + (1 - \lambda) \mathcal{L}^{inter}. \quad (11)$$

²The spatio-temporal branch (*st*) is based on road network traffic information, and thus, is very distinct from the grid modality (*g*). Aligning those two branches empirically degraded the quality of learned trajectory representations.

4.5 Downstream Application

After training, to obtain the final representation \mathbf{z} of a trajectory, we encode the embedding sequence of each branch using the trained trajectory encoder $F_{\theta}^b(\cdot)$ and discard the masking and projection heads:

$$\mathbf{z}^g = F_{\theta}^g(\mathbf{T}^g), \mathbf{z}^r = F_{\theta}^r(\mathbf{T}^r), \mathbf{z}^{st} = F_{\theta}^{st}(\mathbf{T}^{st}). \quad (12)$$

While we aligned branches through the inter-contrastive loss, the embeddings contain their own specific features. Thus, we concatenate all representations to obtain the final trajectory representation $\mathbf{z} \in \mathbb{R}^d$:

$$\mathbf{z} = \mathbf{z}^g || \mathbf{z}^r || \mathbf{z}^{st}. \quad (13)$$

5 EXPERIMENTS

5.1 Experimental Setup

5.1.1 Datasets. We select openly available datasets from Porto³ and San Francisco⁴, containing 1.6 million (July 2013 to June 2014) and 0.6 million (May-June 2008) taxi trajectories, respectively. We extract the corresponding road networks from OpenStreetMap⁵ and map match the trajectories to the road network via Fast Map Matching [32]. We preprocess the trajectory data by pruning trajectories outside the respective city’s bounding box and removing trajectories containing less than 20 points.

5.1.2 Baselines. As baselines, we select several state-of-the-art trajectory representation learning methods that are trained in a self-supervised manner and can be used for various downstream tasks. Thus, we also include those methods proposed for trajectory similarity learning that adopt unsupervised-training, while not considering those methods that are trained supervised, e.g., Traj2SimVec [39], T3S [33] and TrajGAT [37], or need additional labels, e.g., WSCCL [35]. Further, we divide the baselines into two categories, grid-based and road network-based:

Grid-based methods

- t2vec (2018) [15] T2vec encodes cells by sampling a context from neighbor cells and further applying the skip-gram [22] method. The LSTM encoder is trained by inputting a down-sampled and distorted trajectory and then recovering the original trajectory using a seq2seq model.
- CLT-Sim (2022) [7] CLT-Sim pre-trains cell embeddings by treating a grid cell sequence as a sentence and then also applying the skip-gram method. Further the trajectories are encoded using an LSTM and trained using contrastive learning with the NT-Xent loss.
- TrajCL (2023) [2] TrajCL treats the grid as a graph where each cell is connected to its neighbor cells and then utilizing node2vec [10] for pretraining cell embeddings. Further, TrajCL employs a transformer-based encoder and trains it, similar to CLT-Sim in a contrastive fashion.
- CSTTE (2023) [17] CSTTE does not pretrain cells and instead applies an embedding layer, which is trained during the training of the trajectory representations. CSTTE applies

a transformer-based architecture with contrastive learning and NT-Xent loss.

Road network-based methods

- Trembr (2020) [8] Trembr pretrains road embeddings by predicting whether two roads occur on the same trajectory and have the same road type. Further, they apply a seq2seq model to learn trajectory representations, by reconstructing the trajectory and predicting the travel time of each road segment.
- Toast (2022) [5] Toast pretrains road embeddings by applying random walk with skip-gram, similar to [24], and extend it with a road type prediction. Further, they employ a transformer-based architecture and train it by applying a masking objective.
- JCLRNT (2022) [21] CLM does not pretrain road representations and instead encodes roads during the training of the trajectory representations using a GAT [28]. For learning trajectory representations, CLM utilizes contrastive training and proposes to contrast roads to roads, trajectory to trajectory, and trajectory to road.
- START (2023) [13] Similar to CLM, START encodes roads during the training of trajectory representations using GAT and incorporating transfer probabilities between roads. Further, START utilizes a transformer-based encoder and learns trajectory representations using contrastive learning as well as sequence masking.

Additionally, to compare road and grid modality, independently of architecture choices, we add a Transformer baseline that uses contrastive learning with a vanilla Transformer for both modalities (TF^r and TF^g).

5.1.3 Downstream Tasks. We evaluate the performance of TRL methods on three downstream tasks:

- **Trajectory similarity (TS)** aims to find the most similar trajectory in a database D given a query trajectory T_q . To create the *query set* Q and *database* D , we follow Trembr [8] and TrajCL [2]. Specifically, we sample 10,000 trajectories and split them into two sub-trajectories by sampling the odd points of a trajectory T_{odd}^q and its even points T_{even}^q . We insert T_{odd}^q into Q and T_{even}^q into D . To increase the database size, we randomly sample another $k_{neg} = 10,000$ trajectories and add their even samples to D . For evaluation, we take the dot product of a query trajectory $T_q \in Q$ and each trajectory $T \in D$ and rank them by their similarity. Ideally, the even trajectory corresponding to T_q ranks first. We report mean rank (MR) and hit ratio ($HR@1$ and $HR@5$).
- **Travel time estimation (TTE)** predicts the travel time of a trajectory based on its coordinate pairs. It can be used for traffic management, congestion avoidance, or ride-hailing services. We embed each trajectory and train an MLP to predict the travel time in seconds. To avoid information leakage, we only feed the start time and mask all other timestamps for this task. We report the mean absolute error (MAE), mean absolute percentage error ($MAPE$), and root mean squared error ($RMSE$).

³<https://www.kaggle.com/competitions/pkdd-15-taxi-trip-time-prediction-ii>

⁴<https://ieee-dataport.org/open-access/crawdad-epflmobility>

⁵<https://www.openstreetmap.org/>

Table 1: Overall performance of TIGR and baselines. Arrows indicate whether higher values (\uparrow) or lower values (\downarrow) are better. Bold results are the best and underlined results are the second best.

	Task	Trajectory Similarity			Travel Time Estimation			Destination Prediction			
		Metric	MR \downarrow	HR@1 \uparrow	HR@5 \uparrow	MAE \downarrow	MAPE \downarrow	RMSE \downarrow	F ₁ \uparrow	Acc@1 \uparrow	Acc@5 \uparrow
Porto	Road	Transformer	7.604	0.170	0.562	152.83	23.87	222.43	0.084	0.174	0.390
		Trembr	13.74	0.284	0.572	162.32	25.24	236.73	0.118	0.228	0.498
		Toast	31.79	0.026	0.123	176.11	28.23	250.32	<u>0.135</u>	<u>0.256</u>	<u>0.563</u>
		JCLM	<u>1.658</u>	0.773	0.959	145.60	22.43	214.28	0.087	0.179	0.410
		LightPath	1.855	0.739	0.945	156.27	24.25	227.39	0.082	0.171	0.389
		START	2.636	<u>0.808</u>	0.944	129.05	19.73	192.08	0.075	0.158	0.375
	Grid	Transformer	8.134	0.210	0.576	107.78	16.10	168.59	0.081	0.171	0.407
		t2vec	33.10	0.103	0.273	122.65	18.55	185.20	0.084	0.174	0.416
		CLT-Sim	15.87	0.211	0.503	162.62	25.30	241.67	0.098	0.196	0.465
		CSTTE	5.378	0.710	0.820	110.91	16.89	169.59	0.085	0.175	0.423
		TrajCL	1.696	0.789	<u>0.961</u>	<u>96.35</u>	<u>14.31</u>	<u>152.60</u>	0.077	0.162	0.395
	TIGR	1.063	0.959	0.998	83.28	12.67	127.89	0.143	0.266	0.567	
	Improvement	35.89%	18.69%	3.85%	13.57%	11.46%	16.19%	5.93%	3.91%	0.71%	
	San Francisco	Road	Transformer	6.027	0.336	0.727	119.01	22.06	184.98	0.039	0.079
Trembr			17.82	0.193	0.450	121.88	23.00	188.16	0.040	0.081	0.218
Toast			52.14	0.030	0.114	139.16	27.17	209.70	<u>0.055</u>	<u>0.105</u>	0.284
JCLM			<u>1.893</u>	0.728	<u>0.950</u>	108.78	20.07	170.08	0.036	0.075	0.175
LightPath			1.923	0.716	0.946	119.71	22.53	183.62	0.032	0.068	0.178
START			4.153	<u>0.747</u>	0.867	111.83	21.04	172.00	0.030	0.061	0.175
Grid		Transformer	10.69	0.218	0.543	80.12	14.66	133.60	0.038	0.078	0.228
		t2vec	29.19	0.122	0.308	108.32	20.55	164.48	0.051	0.101	<u>0.287</u>
		CLT-Sim	57.10	0.033	0.100	112.98	22.64	173.16	0.051	0.103	0.265
		CSTTE	7.612	0.394	0.704	74.33	14.36	118.25	0.041	0.085	0.231
		TrajCL	4.447	0.673	0.866	<u>67.44</u>	<u>12.51</u>	<u>114.60</u>	0.045	0.090	0.253
TIGR		1.537	0.839	0.972	60.91	11.20	104.32	0.069	0.134	0.340	
Improvement		18.81%	12.32%	2.32%	9.68%	10.47%	8.97%	25.45%	27.62%	18.47%	

- **Destination prediction (DP)** predicts the final destination of a partially observed trajectory. It facilitates route planning, navigation, and recommendation. We embed 90% of each trajectory and train an MLP to predict the final location on the road network. We report the F₁-score (F_1) and accuracy ($Acc@1$ and $Acc@5$).

While some works fine-tune the complete TRL models when training for a downstream task, we follow those that freeze the models and only train a prediction MLP [4, 8, 9, 21].

5.1.4 Implementation Details. We train TIGR using the Adam optimizer with an initial learning rate of 0.001, a batch size of 512, and 10 training epochs. Masking variants are *truncation* and *consecutive masking* for the first set of masking strategies (View 1) and all three for the other set of masking strategies (View 2). We set their parameters to $p_{RM} = p_{TC} = p_{CM} = 0.3$. Dropout is set to 0.1 and the temperature parameter τ to 0.05. We use two encoder layers, a negative sample queue of 2,048, and an embedding dimension of 512. We embed grid cells with a dimension of 256, and road and spatio-temporal branches with a dimension of 128. Similar to previous works [2, 36], we employ node2vec [10] to initialize the grid and road embedding layers. Finally, to balance the loss in Eq. 11, we set $\lambda = 0.5$.

5.2 Experimental Results

5.2.1 Overall Performance. Table 1 reports the overall performance, based on the mean of five different runs with different random seeds. Our proposed method TIGR substantially outperforms all baselines for all metrics on the three downstream tasks and both datasets, demonstrating the benefits of integrating the road-based and grid-based modalities, coupled with the extraction of dynamic spatio-temporal patterns. While TIGR shows substantial improvements in the TTE and DP tasks (up to 16.65% and 10.16% respectively), it demonstrates even greater advancements in the TS task, achieving near-perfect results on both datasets with improvements of up to 43.22%.

To assess robustness in TS, we further increase the task’s difficulty by adding more negative samples k_{neg} (as illustrated in Figure 3). As k_{neg} increases, the performance of all methods declines. Nevertheless, TIGR exhibits a significantly slower rate of decrease, maintaining scores close to 1.0, while the baseline models suffer substantial declines in performance.

These results demonstrate that combining both modalities and including spatio-temporal dynamics substantially benefits all tasks, with the most notable improvements observed in TS. This suggests that grid- and road-modality capture unique trajectory characteristics, with the integration of both enabling more effective and comprehensive trajectory representations than single-modality approaches.

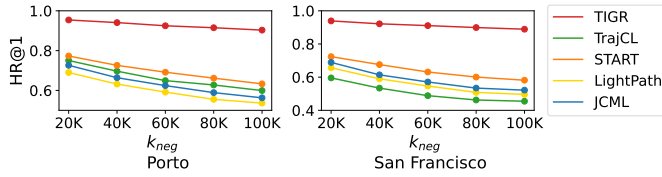


Figure 3: Performance on TS (HR@1 ↑) with increasing amount of negative samples k_{neg} .

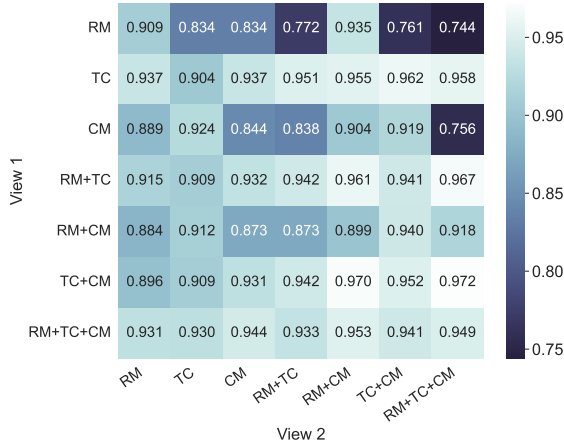


Figure 4: Impact of the masking strategies on the Porto dataset. We report HR@1 (↑) of the TS task.

5.2.2 Comparative Analysis of Modalities. From Table 1, we first compare modalities based on the Transformer baseline, which uses the same architecture for both modalities. On both datasets, road-based TF^r demonstrates superior performance in **TS**, for instance, 30% improvement in terms of MR on Porto. In contrast, grid-based TF^g excels in **TTE**, substantially improving performance compared to TF^r , e.g., 26.2% improvement in terms of MAPE on Porto. This demonstrates, that given the same architecture, both modalities encode unique features and excel at different tasks.

Further, we compare baselines of both modalities⁶ and observe similar trends. For **TTE**, grid-based methods are clearly superior to road-based methods, with TrajCL beating the best road-based method START by 27.5% in terms of MAPE. Even less sophisticated models, such as t2vec, outperform all road-based methods. While JCLRNT and START show improvements by incorporating travel semantics, they only consider static road features and thus cannot capture dynamic spatio-temporal patterns. For **TS**, road-based methods outperform grid-based methods on San Francisco, while on Porto both modalities’ methods are competitive. For **DP**, the performance disparity between modalities is less pronounced, indicating that both modalities capture relevant features for this task. Our comparative analysis reveals that road-based and grid-based modalities exhibit complementary strengths across different trajectory

⁶Note that previous works which compared to methods of the other modality, adapted them to their modality [13, 21], e.g., using TF^r as input instead of TF^g .

Table 2: Ablation study on the Porto dataset.

	TS	TTE	DP
	HR@1 ↑	MAPE ↓	Acc@1 ↑
w/o grid-branch	0.958	18.71	0.223
w/o road-branch	0.923	13.33	0.182
w/o ST-branch	0.874	13.88	0.240
w/o inter-loss	0.973	13.22	0.214
w/o LMA	0.963	13.30	0.236
w/o RoPE	0.973	12.94	0.236
TIGR	0.976	12.76	0.241

tasks, emphasizing their respective strengths in capturing distinct aspects of trajectory data.

5.2.3 Ablation Study. In our ablation study, we leave out one module at a time to see its effects. Table 2 reports the results, demonstrating that each module contributes to the performance of TIGR. Removing the grid-branch significantly impacts the **TTE** task increasing MAPE by 46.8%, again suggesting that the grid-modality is crucial for accurate travel time predictions. Excluding the road-branch notably reduces **DP** performance, indicating the importance of road network topology. The spatio-temporal (ST) branch proves vital, with its removal causing the most significant decrease in **TS** performance (10.9% relative drop in HR@1), underlining the importance of modeling temporal dynamics. The inter-loss, Local Multi-head Attention (LMA), and Rotary Position Embedding (RoPE) additionally contribute to TIGR’s performance, with their removal causing slight decreases across all metrics. These results demonstrate that all components of our architecture contribute to the overall performance, with the grid, road, and spatio-temporal branches playing crucial roles in various aspects of trajectory representation learning.

5.2.4 Impact of masking strategies. We study the impact of masking methods by varying masking strategies applied to each view on the **TS** task on Porto. We utilize random masking (RM), truncation (TC), and consecutive masking (CM) and their combinations and report the results in Figure 4. Masking significantly impacts the downstream performance, with an improvement of 25.4% between the least and best-performing combinations. Only the *anchor encoder* processing the trajectories modified by View 1 masking (presented on the y-axis) is trained through gradient descent. To this extent, we observe that masking applied to View 1 has a greater impact on performance. More specifically, TC is the best individual masking strategy, and combinations containing TC are superior to those without it. Further, using only one masking strategy per view, as done by previous TRL methods [2, 13], is inferior to using a combination of masking strategies for each view. Finally, based on the best-performing combination, we select TC and CM for View 1 and all three for View 2.

5.2.5 Comparison of Top-500 Similar Trajectories. To provide a visual comparison of similar trajectory search results, we present the 500 most similar trajectories retrieved by TIGR, START, and TrajCL for a given query trajectory in Figure 5. The query trajectory (depicted in red) originates from Porto’s main station, traverses the



Figure 5: Given the query trajectory (red), we visualize the 500 most similar trajectories retrieved by TIGR (left), START (middle) and TrajCL (right).

highway, and ends in the coastal area. TIGR demonstrates significantly higher overlap between retrieved trajectories and the query trajectory. Minor deviations are primarily observed in the coastal region, suggesting that TIGR predominantly identifies trajectories that originate from the main station and terminate at various specific locations within the coastal area. In contrast, similar trajectories retrieved by START and TrajCL exhibit substantially less overlap with the query trajectory. While these trajectories generally maintain connectivity with the query path, they cover different areas along the route. These findings further illustrate that the integration of grid and road modalities enhances the modeling of intricate and diverse trajectory characteristics, thereby facilitating the retrieval of highly similar trajectories.

6 CONCLUSION

In this paper, we introduced TIGR, a novel trajectory representation learning model that effectively integrates road and grid modalities while incorporating spatio-temporal dynamics. Our comprehensive experiments on two real-world datasets demonstrate TIGR's superior performance, outperforming baselines substantially, i.e., up to 43.22% for trajectory similarity, up to 16.65% for travel time estimation, and up to 10.16% for destination prediction. Moreover, we conducted the first comprehensive comparison between grid and road modalities, revealing their distinct strengths in different tasks. These findings emphasize the potential of combining grid and road modality and the importance of capturing dynamic spatio-temporal patterns of urban traffic.

REFERENCES

- [1] Mahmoud Assran, Mathilde Caron, Ishan Misra, Piotr Bojanowski, Florian Bordes, Pascal Vincent, Armand Joulin, Mike Rabbat, and Nicolas Ballas. 2022. Masked Siamese Networks for Label-Efficient Learning. In *17th European Conference on Computer Vision ECCV*.
- [2] Yanchuan Chang, Jianzhong Qi, Yuxuan Liang, and Egemen Tanin. 2023. Contrastive Trajectory Similarity Learning with Dual-Feature Attention. In *39th IEEE International Conference on Data Engineering, ICDE 2023*. IEEE, 2933–2945.
- [3] Pingfu Chao, Yehong Xu, Wen Hua, and Xiaofang Zhou. 2020. A Survey on Map-Matching Algorithms. In *31st Australasian Database Conference, ADC*, Vol. 12008. Springer, 121–133.
- [4] Ting Chen, Simon Kornblith, Mohammad Norouzi, and Geoffrey Hinton. 2020. A simple framework for contrastive learning of visual representations. In *International Conference on Machine Learning, ICML*. PMLR, 1597–1607.
- [5] Yile Chen, Xiucheng Li, Gao Cong, Zhifeng Bao, Cheng Long, Yiding Liu, Arun Kumar Chandran, and Richard Ellison. 2021. Robust Road Network Representation Learning: When Traffic Patterns Meet Traveling Semantics. In *ACM International Conference on Information and Knowledge Management, CIKM*. ACM, 211–220.
- [6] Zhen Chen, Dalin Zhang, Shanshan Feng, Kaixuan Chen, Lisi Chen, Peng Han, and Shuo Shang. 2024. KGTS: Contrastive Trajectory Similarity Learning over Prompt Knowledge Graph Embedding. In *Thirty-Eighth Conference on Artificial Intelligence, AAAI*.
- [7] Liwei Deng, Yan Zhao, Zidan Fu, Hao Sun, Shuncheng Liu, and Kai Zheng. 2022. Efficient Trajectory Similarity Computation with Contrastive Learning. In *31st ACM International Conference on Information & Knowledge Management, CIKM*. ACM, 365–374.
- [8] Tao-Yang Fu and Wang-Chien Lee. 2020. Trembr: Exploring Road Networks for Trajectory Representation Learning. *ACM Trans. Intell. Syst. Technol.* 11, 1 (2020).
- [9] Jean-Bastien Grill, Florian Strub, Florent Althé, Corentin Tallec, Pierre H. Richemond, Elena Buchatskaya, Carl Doersch, Bernardo Ávila Pires, Zhaohan Guo, Mohammad Gheshlaghi Azar, Bilal Piot, Koray Kavukcuoglu, Rémi Munos, and Michal Valko. 2020. Bootstrap Your Own Latent - A New Approach to Self-Supervised Learning. In *Annual Conference on Neural Information Processing Systems 2020, NeurIPS*.
- [10] Aditya Grover and Jure Leskovec. 2016. node2vec: Scalable Feature Learning for Networks. In *KDD*.
- [11] Kaiming He, Xinlei Chen, Saining Xie, Yanghao Li, Piotr Dollár, and Ross B. Girshick. 2022. Masked Autoencoders Are Scalable Vision Learners. In *IEEE/CVF Conference on Computer Vision and Pattern Recognition, CVPR 2022*. IEEE, 15979–15988.
- [12] Neal Jean, Sherrie Wang, Anshul Samar, George Azzari, David Lobell, and Stefano Ermon. 2019. Tile2vec: Unsupervised representation learning for spatially distributed data. In *Proceedings of the AAAI Conference on Artificial Intelligence*, Vol. 33. 3967–3974.
- [13] Jiawei Jiang, Dayan Pan, Houxing Ren, Xiaohan Jiang, Chao Li, and Jingyuan Wang. 2023. Self-supervised Trajectory Representation Learning with Temporal Regularities and Travel Semantics. In *39th IEEE International Conference on Data Engineering, ICDE 2023*. IEEE, 843–855.
- [14] Guangyin Jin, Huan Yan, Fuxian Li, Yong Li, Jincai Huang Additional, and Jincai Huang. 2023. Dual Graph Convolution Architecture Search for Travel Time Estimation. *ACM Transactions on Intelligent Systems and Technology* (2023).
- [15] Xiucheng Li, Kaiqi Zhao, Gao Cong, Christian S. Jensen, and Wei Wei. 2018. Deep Representation Learning for Trajectory Similarity Computation. In *34th IEEE International Conference on Data Engineering, ICDE 2018*. IEEE Computer Society, 617–628.
- [16] Yan Lin, Huaiyu Wan, Shengnan Guo, Jilin Hu, Christian S. Jensen, and Youfang Lin. 2023. Pre-Training General Trajectory Embeddings With Maximum Multi-View Entropy Coding. *IEEE Transactions on Knowledge and Data Engineering* (2023).
- [17] Yan Lin, Huaiyu Wan, Shengnan Guo, and Youfang Lin. 2022. Contrastive Pre-training of Spatial-Temporal Trajectory Embeddings. *CoRR* abs/2207.14539 (2022).
- [18] Yang Liu, Ruo Jia, Jieping Ye, and Xiaobo Qu. 2022. How machine learning informs ride-hailing services: A survey. *Communications in Transportation Research* 2 (2022), 100075.
- [19] Zhipeng Ma, Zheyuan Tu, Xinhai Chen, Yan Zhang, Deguo Xia, Guyue Zhou, Yilun Chen, Yu Zheng, and Jiangtao Gong. 2024. More Than Routing: Joint GPS and Route Modeling for Refine Trajectory Representation Learning. In *Proceedings of the ACM Web Conference, WWW*. ACM.
- [20] Gengchen Mai, Krzysztof Janowicz, Bo Yan, Rui Zhu, Ling Cai, and Ni Lao. 2020. Multi-Scale Representation Learning for Spatial Feature Distributions using Grid Cells. In *8th International Conference on Learning Representations, ICLR*. OpenReview.net.
- [21] Zhenyu Mao, Ziyue Li, Dedong Li, Lei Bai, and Rui Zhao. 2022. Jointly Contrastive Representation Learning on Road Network and Trajectory. In *31st ACM International Conference on Information & Knowledge Management, CIKM*. ACM, 1501–1510.
- [22] Tomáš Mikolov, Kai Chen, Greg Corrado, and Jeffrey Dean. 2013. Efficient Estimation of Word Representations in Vector Space. In *1st International Conference*

- on Learning Representations, *ICLR*.
- [23] Aäron Oord et al. 2018. Representation Learning with Contrastive Predictive Coding. *CoRR* abs/1807.03748 (2018).
- [24] Bryan Perozzi, Rami Al-Rfou, and Steven Skiena. 2014. DeepWalk: online learning of social representations. In *ACM SIGKDD*. ACM, 701–710.
- [25] Ashutosh Sao, Simon Gottschalk, Nicolas Tempelmeier, and Elena Demidova. 2023. MetaCitta: Deep Meta-Learning for Spatio-Temporal Prediction Across Cities and Tasks. In *27th Pacific-Asia Conference on Knowledge Discovery and Data Mining, PAKDD 2023*. Springer, 70–82.
- [26] Jianlin Su, Yu Lu, Shengfeng Pan, Bo Wen, and Yunfeng Liu. 2021. RoFormer: Enhanced Transformer with Rotary Position Embedding. *CoRR* abs/2104.09864 (2021).
- [27] Ashish Vaswani, Noam Shazeer, Niki Parmar, Jakob Uszkoreit, Llion Jones, Aidan N. Gomez, Lukasz Kaiser, and Illia Polosukhin. 2017. Attention is All you Need. In *Annual Conference on Neural Information Processing Systems, NeurIPS*. 5998–6008.
- [28] Petar Velickovic, Guillem Cucurull, Arantxa Casanova, Adriana Romero, Pietro Liò, and Yoshua Bengio. 2018. Graph Attention Networks. In *ICLR 2018*. OpenReview.net.
- [29] Meng-xiang Wang, Wang-Chien Lee, Tao-Yang Fu, and Ge Yu. 2021. On Representation Learning for Road Networks. *ACM Trans. Intell. Syst. Technol.* 12, 1 (2021), 11:1–11:27.
- [30] Ning Wu, Wayne Xin Zhao, Jingyuan Wang, and Dayan Pan. 2020. Learning Effective Road Network Representation with Hierarchical Graph Neural Networks. In *26th ACM SIGKDD Conference on Knowledge Discovery and Data Mining, KDD*. ACM, 6–14.
- [31] Yanxin Xi, Tong Li, Huandong Wang, Yong Li, Sasu Tarkoma, and Pan Hui. 2022. Beyond the first law of geography: Learning representations of satellite imagery by leveraging point-of-interests. In *Proceedings of the ACM Web Conference, WWW*. 3308–3316.
- [32] Can Yang and Gyözö Gidófalvi. 2018. Fast map matching, an algorithm integrating hidden Markov model with precomputation. *Int. J. Geogr. Inf. Sci.* 32, 3 (2018), 547–570.
- [33] Peilun Yang, Hanchen Wang, Ying Zhang, Lu Qin, Wenjie Zhang, and Xuemin Lin. 2021. T3S: Effective Representation Learning for Trajectory Similarity Computation. In *37th IEEE International Conference on Data Engineering, ICDE*. IEEE, 2183–2188.
- [34] Sean Bin Yang, Chenjuan Guo, Jilin Hu, Jian Tang, and Bin Yang. 2021. Unsupervised Path Representation Learning with Curriculum Negative Sampling. In *30th International Joint Conference on Artificial Intelligence, IJCAI*, Zhi-Hua Zhou (Ed.). ijcai.org.
- [35] Sean Bin Yang, Chenjuan Guo, Jilin Hu, Bin Yang, Jian Tang, and Christian S. Jensen. 2022. Weakly-supervised Temporal Path Representation Learning with Contrastive Curriculum Learning. In *38th IEEE International Conference on Data Engineering, ICDE*. IEEE.
- [36] Sean Bin Yang, Jilin Hu, Chenjuan Guo, Bin Yang, and Christian S. Jensen. 2023. LightPath: Lightweight and Scalable Path Representation Learning. In *29th ACM SIGKDD Conference on Knowledge Discovery and Data Mining, KDD 2023*. ACM.
- [37] Di Yao, Haonan Hu, Lun Du, Gao Cong, Shi Han, and Jingping Bi. 2022. TrajGAT: A Graph-based Long-term Dependency Modeling Approach for Trajectory Similarity Computation. In *28th ACM SIGKDD Conference on Knowledge Discovery and Data Mining, KDD*. ACM, 2275–2285.
- [38] Biao Zhang and Rico Sennrich. 2019. Root Mean Square Layer Normalization. In *Annual Conference on Neural Information Processing Systems, NeurIPS*. 12360–12371.
- [39] Hanyuan Zhang, Xinyu Zhang, Qize Jiang, Baihua Zheng, Zhenbang Sun, Weiwei Sun, and Changhu Wang. 2020. Trajectory Similarity Learning with Auxiliary Supervision and Optimal Matching. In *29th International Joint Conference on Artificial Intelligence, IJCAI*. ijcai.org, 3209–3215.
- [40] Wanyi Zhou, Xiaolin Xiao, Yue-Jiao Gong, Jia Chen, Jun Fang, Naiqiang Tan, Nan Ma, Qun Li, Hua Chai, Sang-Woon Jeon, and Jun Zhang. 2023. Travel Time Distribution Estimation by Learning Representations Over Temporal Attributed Graphs. *IEEE Trans. Intell. Transp. Syst.* 24, 5 (2023), 5069–5081.